

Additional file 1

(Supporting Information)

Geological structures controlled the rupture process of the 2011 Tohoku-Oki earthquake in the Northeast Japan Arc

Kei Baba^{a*}, Takeyoshi Yoshida^{b*}

a 2-29-12 Ichikawa, Ichikawa-Shi, 272-0034, Japan., kei-baba@mvj.biglobe.ne.jp

*b Department of Earth Science, Graduate School of Science, Tohoku University, 6-3 Aza-Aoba,
Aramaki, Aoba-ku, Sendai 980-8578, Japan, tyoshida@m.tohoku.ac.jp*

*Corresponding author: Takeyoshi Yoshida.

1. Stratigraphy

The geological ages of the interpreted seismic units were determined by using 14 MITI/METI exploratory well and 14 DSDP/ODP well data (Baba, 2017).

1.1 Northeast Japan forearc

By applying the seismic stratigraphic technique to the Northeast (NE) Japan forearc, we

identified nine seismic units bounded by tectonic-induced onlap surfaces above the pre-Cretaceous basement rocks (Baba, 2017). From bottom to top, basement rocks (pre-Cretaceous accretionary prism complex, igneous rocks and metamorphic rocks), Cr unit (Early Cretaceous to Early Eocene sediments), P2 unit (Middle Eocene to Early Oligocene sediments), P1 unit (Late Oligocene to Early Miocene sediments), N6 unit (c.17 to 13.5 Ma sediments), N5 unit (13.5 to c.10.5 Ma sediments), N4 unit (c.10.5 to c.6.0 Ma sediments), N3 unit (c.6.0 to c.3.6 Ma sediments), N2 unit (c.3.6 to c.1.8 Ma sediments), and N1 unit (c.1.8 Ma to recent sediments; see Fig.S1). The ages of c.17 Ma and 13.5 Ma correspond to the beginning of the Climax Syn-rift Stage and the end of the Late Syn-rift Stage (Japan Sea opening period), respectively. The ages of c.10.5, c.6.0, c.3.6 and c.1.8 Ma are the prominent constructive tectonic events by which the tectonic-induced onlap was formed (Baba, 2017). Of these ages, the tectonic events of c.10.5, c.6.0, c.3.6 Ma, and c.1.8 Ma correspond to the changes in motion of the Pacific Plate (ex. Jackson et al., 1975; Northrup et al., 1995; Austermann et al., 2011, Harbert and Cox, 1989; Otsuki, 1982, 1986; Baba, 2017). The geological time scale used in this study was based on Gradstein et al. (2012).

1.2 NE Japan backarc

We identified four seismic units bounded by tectonic-induced onlap surface above the acoustic

basement (Baba, 2017). From bottom to top, they are Yt4 unit (Syn-rift Stage sediments of Early Miocene age to 13.5 Ma), Yt3 unit (13.5 to c.3.6 Ma sediments), Yt2 unit (c.3.6 to c.1.8 Ma sediments), and Yt1 units (c.1.8 Ma to recent sediments; see Fig.S1). The acoustic basement is composed of pre- to syn-rift volcanic / volcanoclastic rocks and Pre-Paleogene sedimentary and plutonic rocks. After the Syn-rift Stage, the backarc region was tectonically stable (13.5–c.3.6 Ma), but after c.3.6 Ma, this region changed into a strong compression field characterized by the tectonic inversion of half grabens (the Dewa Disturbance of Huzioka (1968)).

2. Time-depth contour map of surrounding ocean area of the NE Japan and the typical seismic sections.

In the seismic interpretation, the author traced the large transcurrent faults recognizing large flower structure (arrow marks at top of the seismic sections in Figs. S3A and S3B), The flower structure is characterized by the fault array resembling the structure of the petals of a flower in cross section, and the location and width of the large transcurrent faults are shown by arrow marks at the top of the seismic sections in Figs. S3A and S3B. They were traced carefully on E-W and N-S 2D seismic sections by recognizing their characteristic fault array, and were checked carefully the connectivity to the tectonic lines marked on the geological map of NE Japan land area. In the case of

Fault T, the characteristic and large-scale flower structure showing a few tens kilometer width, the relatively high 2D seismic line intervals and the nearshore 2D seismic lines helped us to interpret the main fault and their branched fault system, and in the case of Fault F, the 3D seismic data recorded around the Offshore Hidaka and the Offshore Sanriku Basin supported us in the more accurate seismic interpretation.

Fig.S2 is a time-depth contour map of the top of the P1 seismic stratigraphic unit in the forearc region and the top of the acoustic basement in the backarc region of the NE Japan Arc. The geological age of this map corresponds approximately to the start of the Climax Syn-rift stage (see Fig. S1). In Fig. S2, the fault system on land shows only the significant half-graben listric faults and large strike-slip faults (transcurrent faults). and was based on GeomapNavi of Geological Survey of Japan (<https://gbank.gsj.jp/geonavi/geonavi.php>), Japan Natural Gas Association • Japan offshore petroleum development association (1992) and Takahashi (2006). Almost all the faults shown in Fig. S2 were formed during Syn-rift Stage, but were inverted by regional compressional stress that started around 10Ma (Fig. S1).

On seismic sections, the NW-SE trending large transcurrent faults are characterized by the development of large and distinct flower structures as shown in Figs. S3A and S3B, that are connected to those on land (see Fig. S2). Especially, Fault I connects to the Honjo-Sendai tectonic

line (Taguchi, 1960) with NW-SE trending graben, and Faults T to N play a role to protrude Block F southeastwardly along them. However, the connection of Fault G is uncertain on the southwestern side of the Offshore Hidaka Basin (Fig. S2).

In the forearc region, Faults B to F, Fault G, Fault H, and Faults T to N terminate trenchward forming leading extensional imbricate fan with sinistral sense. Conversely, Fault I and P terminate trenchward forming with tailing extensional imbricate fan with dextral sense. The current lateral displacements basically maintain those occurred in early stage of Japan Sea spreading (Baba, 2017). With the progress of the spreading, the inversion of strike-slip direction occurred along Fault I (Hoshi and Takahashi, 1999) and Faults T to N (Awaji et al., 2006). Particularly, the inversion of Fault I caused transcompressional deformation to the Abukuma Ridge and the Offshore Joban Basin in which a branched fault system of imbricate fan developed. The cause of this strike-slip inversion will be described in Section 3. In the southern end of the NE Japan Arc, the Fossa Magna pull-apart basin (Baba, 2017) extends from the east end of the Yamato Rise to the Fossa Magna through the Toyama Trough (Fig. S2), and both its margins are bounded by right-stepping right lateral faults (Faults P and R) that exhibit large and distinct flower structure (Line 11 of Fig. S3B). This right-lateral basin structural pattern fits well with the pull-apart basin model composed of a series of small pull-apart depressions shown in Fig.13A of Ten Brink and Ben-Avraham (1989). This

right-lateral motion is thought to be caused by "double-door opening " (Otofujii et al., 1985) or "double saloon door opening" (Martin, 2011) of Japan Sea during the Early to Middle Miocene.

The north end of the NE Japan Arc is bounded by the left-lateral fault zone (Faults B to F) associated with the large pull-apart basin (Offshore Hidaka Basin). The Offshore Hidaka Basin is an asymmetric basin deeply dipping north toward Fault A. The master faults of this pull-apart basin are Fault B and F. This basin structural-pattern fits well with the asymmetric pull-apart basin model of Ten Brink and Ben-Avraham (1989). The formation of the basin is thought to have started in the Climax Syn-rift Stage (c.13.5-17Ma), because N6 unit reflectors appear to onlap against top of Late Oligocene-Early Miocene P1 unit dipping northeastward (see Fig. S1 and Line1 of Fig. S3A).

The backarc rift system of the NE Japan Arc is composed of NE-SW to NNE-SSW trending half grabens that are cut by the NW-SE trending large transcurrent faults described above, and are inverted by strongly contractive stress which occurred at c.3.6 Ma (Okamura, 2000; Baba, 2017 etc.). In the backarc rift system, there are four large rift basins. They are, from north to south, the Nishitsugaru Basin (L), the Akita–Yamagata Basin (M), the Niigata Basin (O), and the Sado Basin (S) (Fig. S2). Along these large rift basins, the backarc half-graben system exhibits the following tectonic features: i) on the west side of the four large rift basins, half-grabens are formed by westward-dipping listric faults, in contrast, ii) on the east side of the four large rift basins,

half-grabens are formed by eastward-dipping listric faults (see Fig. S2). Such orientation patterns of half grabens are a good fit with the double detachment fault model of Lister et al. (1986). According to this model, the orientation pattern was formed by two long detachment faults that moved in the opposite direction (detachment Fault 1 and 2 in Fig. S4), and the four large rift basins correspond to the largest spreading part formed by detachment Fault 2, and the Japan Basin corresponds to the largest spreading part formed by detachment Fault 1. In contrast, the backarc rift system of the Southwest (SW) Japan Arc is characterized by NE-SW trending large horsts and grabens such as the Kita-Yamato Bank, the Kita-Yamato Trough, the Yamato Rise, the Kita-Oki Bank, the Yamato Basin, the Oki Bank, and the Oki Trough (see Figs S2). Such tectonic architecture may be explained by applying the “Simple shear model (Lister et al., 1986)” or “Continental fragmentation (Cogne and Humler, 2008)”. On the west side of this backarc rift system, the Japan Basin spread widely as a backarc basin characterized by a thick pile of subaqueous basaltic lava flows erupted during the Syn-rift Stage.

3. Dimension of the large transcurrent faults in the Northeast Japan Arc

In this section, we explain the maximum cross-strike width, total length, lateral displacement and fault movement history of large transcurrent faults by referring Fig. 1, Fig. S2 and Fig. S5. The

maximum cross-strike width was measured at point indicated by red arrows in Fig. S2, and the total length was measured from the large transcurrent faults illustrated in Fig.1. The lateral displacement was simply measured from the amount of lateral shift of Fault E (the western margin fault of the backarc rift system) at the intersection point with large transcurrent fault recognized in Fig. 1. Because the marginal fault on the Eurasian continent side of the Japan Basin exhibits an approximately straight, smooth line (see Fig. 1). These values represent essentially the state at the end of the Syn-rift Stage as shown in Fig. S5.

In the following, we consider that left-lateral motion of the large transcurrent faults occurred during the Syn-rift Stage was caused by adjusting for the difference in backarc spreading rate which increased toward the south of the Japan Sea (Baba, 2017).

(1) Faults A, B, C, and F (Offshore Hidaka tectonic line): c.100km of left-lateral displacement is estimated. The maximum cross-strike width of the fault zone is c.15km, and the total length is c.1000 km. However, more than 200 km of right-lateral strike-slip movement caused by the Kuril Basin opening in the Upper Oligocene was assumed along these faults (Kurita and Yokoi, 2000; Itoh and Tsuru, 2006).

(2) Fault G (Offshore Sanriku tectonic line): c.70 km of left-lateral displacement is estimated. The maximum cross-strike width of the fault zone is c.10 km, and total length is c.850 km. The fault

activity before the Pre-rift Stage is unknown.

(3) Fault H (Hizume-Kesenuma Fault): c.20 km of left-lateral displacement is estimated. The maximum cross-strike width of the fault zone is c.10 km, and the total length is c.650km. This fault was originally formed by the Oshima Orogeny that occurred during the Early Cretaceous, and c.40 km of left-lateral displacement was estimated (Otsuki and Ehiro, 1992).

(4) Fault I (Honjo-Sendai tectonic line): c.80 km of left-lateral displacement is estimated. The maximum cross-strike width of the fault zone is c.20 km, and the total length is c.650km. However, at the start of the Early Rift Stage, paleomagnetic evidence suggests right-lateral movement of more than 20 km along the Chokai-Ishinomaki tectonic line which is one of the lateral faults comprising Fault I, and this right-lateral motion is thought to be caused by anticlockwise rotation of the NE Japan on the northern side of Fault I (Hoshi and Takahashi, 1999). In backbone range of the NE Japan, the Honjo-Sendai tectonic line approximately matches with the Onikobe-Yuzawa Mylonite Zone which was formed by the Oshima Orogeny during the Late Cretaceous and by left-lateral movement (Otsuki and Ehiro, 1992). Therefore, this tectonic line may be formed originally by left-lateral motion during the Late Cretaceous.

(5) Faults T to N (Miomote-Tanakura tectonic lines): c.40 km of right-lateral displacement is estimated. The maximum cross-strike width of the fault zone is c.10 km, and the total length is c.650

km. However, during the Early and Climax Rift Stage, structural geological evidence suggests the existence of left-lateral motion along the tectonic line. The amount of the left-lateral motion is unknown (Awaji et al., 2006). The reversion of the strike-slip direction is considered to be caused by collision of the Izu-Bonin Arc with central Japan starting at 15Ma (Awaji et al., 2006; Baba, 2017). This fault was originally formed by oblique subduction of the Izanagi plate during the late to middle Upper Cretaceous, and was reactivated during the late Early to late Late Eocene, and 240km of left-lateral motion was proposed (Otsuki and Ehiro, 1992).

(6) Fault P (Kashiwazaki-Choshi tectonic line): c.200 km of right-lateral displacement is estimated. The total length is c.900km and the maximum cross-strike width of the fault zone is c.15km around the eastern end of the fault zone. This right-lateral motion is thought to be caused by "double-door opening " (Otofuji et al., 1985) or "double saloon door opening" (Martin, 2011) of Japan Sea during the Early to Middle Miocene.

4. Earthquake distribution before the 2011 Tohoku-Oki earthquake

Fig. S6 shows the distribution of earthquakes with a magnitude greater than Mj 4.0 from March 9, 1931 to March 8, 2011 (from JMA earthquake catalog). The purpose of this section is to explain the outline the seismic distribution, so we did not explain the interplate, upper plate and lower plate

earthquakes separately. The dense distribution of earthquakes along the NE Japan forearc is confined between Fault T and Fault F with their imbricate fan. The linear arrangement of earthquake hypocenters is recognized along the forearc side of Fault P, and a relatively dense distribution of earthquakes is observed along Faults A, C, and F. Such a relatively dense distribution is also found in the forearc region near and along Fault I and Fault H. On the southern side of Fault I, a dense distribution zone of earthquakes roughly corresponds to the Abukuma Ridge, in which numerous trench-parallel faults have developed. On the north side of Fault H, a relatively low-density distribution of earthquakes extends widely along the NE Japan forearc. On the backarc side, earthquake hypocenters shallower than 30 km are concentrated along Fault E, which forms a boundary between the backarc rift system and the Japan Basin. The southern limit of this concentrated earthquake zone is clearly bounded by Fault N. Therefore, Faults T to N are of great importance as the southern limit of the dense distribution of earthquakes in both the forearc and backarc of the NE Japan Arc.

5. Tectonic control of the rupture propagation process

Fig. 5S shows the rupture propagation models by using snapshots obtained from teleseismic data (Yagi and Fukahata, 2011; Shao et al., 2011), strong motion data (Yoshida, Y. et al., 2011;

Yoshida K. et al., 2011), and tsunami plus strong motion data (Koketus et al., 2011; Lee et al., 2011).

The rupture process common to these studies listed in Fig. S7 can be summarized as follows: The weak rupture initiated in Block C and then gradually propagated trenchward of Block C and D. At approximately 60-80 s, the coseismic slip spreads toward Block B and reached the maximum slip in Blocks B, C, and D. Subsequently, the coseismic slip decreased gradually, while at the same time a weak slip region began to move southwestward in Block E. At approximately 100 s, the slip region almost disappeared in Blocks C and D, and at approximately 120 s, the rupture process of the mainshock had finished.

6. Back slip rate distribution

Fig. S8 shows the distribution of the back slip rate estimated from the geodetic inversion using horizontal and vertical site velocity data (Suwa et al., 2006). In this figure, we can see the large left-lateral shift of the distribution of the back slip rate along Faults A, B, C, and F. We can also see the cutoff of the southern margin of the distribution of the back slip rate (6~10 cm/yr) by Faults T to N. In general, a large back slip rate means a strong interplate coupling (Suwa et al., 2006), therefore, such a distribution pattern of the back slip rate is considered to represent the changes in interplate coupling controlled by large transcurrent faults. In addition, the western margin of distribution of the

back slip rate shifts laterally at the intersection point with the following transcurrent faults: i) Faults A, B, C, and F or Fault G (left lateral), ii) Fault I (left lateral), and iii) Fault P (right lateral). This western margin has been assumed to be the landward downdip limit of the transition zone of the locked fault zone on the plate boundary that extends down to a depth of about 100 km (Suwa et al., 2006). This shift pattern is almost concordant with that of the downdip limit of interplate earthquakes (Green dashed line in Fig. S8) that has been considered to be a western margin of the locked fault zone on the plate boundary, and its landward downdip limit has been estimated from interplate seismicity to be at a depth of approximately 60 km (Igarashi et al., 2001; Kita et al., 2010; Uchida and Matsuzawa, 2013). As described above, it is clear that the distribution of the back slip rate (interplate coupling) along the NE Japan Arc is strongly controlled by the large transcurrent faults. Furthermore, the changes in the western margin of the distribution of the back slip rate corroborate that these transcurrent faults could deeply penetrate the mantle or crosscut the entire lithosphere as described in Section 2.3.

References

Austermann, J., Z. Ben-Avraham, P. Bird, O. Heidbach, G. Schubert, & J. M. Stock [2011]

Quantifying the forces needed for the rapid change of Pacific plate motion at 6 Ma, *Earth Planet. Sci. Lett.*, 307, 289-297, doi: 10.1016/j.epsl.2011.04.043.

Awaji, D., Yamamoto, D. and Takagi, H. (2006) Kinematic history of the Tanakura shear zone at brittle regime. *Jour. Geol. Soc. Japan*, 112, 222-240 (in Japanese with English abstract).

Baba, K (2017) Marine geology (Chapter 10) in *Regional Geology of Japan 2, Tohoku District* (Nihon Chiho Chishitsushi 2 Tohoku Chiho) edited by Geological Society of Japan. Asakura Publishing Co., Ltd., 427-478, ISBN 978-4-254-16782-5 (in Japanese).

Cogne, J.-P. and Humler, E. (2008) Global scale patterns of continental fragmentation: Wilson's cycles as a constraint for long-term sea-level changes. *Earth Planet. Sci. Lett.*, 273, 251-259.

Gradstein, F.M., Ogg, J. G., Schmits M, and Ogg, G. (2012) *The geologic time scale 2012* 1st edition. Elsevier.

Harbert, W. and Cox, A., 1989, Late Neogene of the Pacific plate. *Journal of Geophysical Research*, 94, 3056-3064.

Hoshi, H. and Takahashi, M. (1999) Miocene counterclockwise rotation of Northeast Japan: a review and new model. *Bull. Geol. Surv. Japan*, 50, 3-16.

Huzioka, K. (1968) The Dewa Disturbance in Akita Oil-field. *Japan Assoc. Petrol. Tech.*, 33(5),

283-297, doi;<https://doi.org/10.3720/japt.33.283>.

Igarashi, T., Matsuzawa, T., Umino, N. and Hasegawa, A. (2001) Spatial distribution of focal mechanisms for interplate and intraplate earthquakes associated with the subducting Pacific plate beneath the northeastern Japan arc: A triple-planed deep seismic zone. *Jour. Geophys. Res.*, 106, B2, 2177-2191.

Itoh, Y. and Tsuru, T. (2006) A model of late Cenozoic transcurrent motion and deformation in the fore-arc of northeast Japan: Constraints from geophysical studies. *Physics of the Earth and Planetary Interiors*, 156, 117-129.

Iwasaki, T., Kato, W., Moriya, T., Hasemi, A., Umino, N., Okada, T., Miyashita, T., Mizogami, K., Takeda, T., Sekine, S., Matsushima, T., Tashiro, K. and Miyamachi, H. (2001) Extensional structure on northern Honshu Arc as inferred from seismic refraction/wide-angle reflection profiling, *Geophys. Res. Lett.*, 28, 2329-2332.

Jackson, E.D., Shaw, H.R. and Bargar, K.E. (1975) Calculated geochronology and stress field orientations along the Hawaiian Chain. *Earth and Planet. Sci. Lett.*, 26, 145-155.

Japan Natural Gas Association • Japan offshore petroleum development association (1992) Oil and natural gas resources in Japan. 4-58. Japan Natural Gas Association • Japan offshore petroleum development association, Tokyo (in Japanese).

Kita, S., Okada, T., Hasegawa, A., Nakajima, J. and Matsuzawa, T. (2010) Existence of interplane earthquakes and neutral stress boundary between the upper and lower planes of the double seismic zone beneath Tohoku and Hokkaidou, northeastern Japan. *Tectonophysics*, 496, 68-82.

Koketsu, K., Yokota, Y., Nishimura, N., Yagi, Y., Miyazaki, S., Satake, K., Fujii, Y., Miyake, H., Sakai, S., Yamanaka, Y. and Okada, T. (2011) A unified source model for the 2011 Tohoku earthquake. *Earth Planet. Sci. Lett.*, 310, 480-487.

Kurita, Y. and Yokoi, s. (2000) Cenozoic tectonic settings and current exploration concept in southern central Hokkaido, northern Japan. *Jour. Assoc. Petrol. Tech. Japan*. 65(1), 58-70 (in Japanese with English abstract).

Lee, S-J., Huang, B-S., Ando, M., Chiu, H-C. and Wang, J-H. (2011) Evidence of large scale repeating slip during the 2011 Tohoku-Oki earthquake. *Geophy. Res. Lett.*, 38, L19306, doi:10.1029/2011GL049580.

Lister, G.S., Etheridge, M.A. and Symonds, P.A. (1986) Detachment faulting and the evolution of passive continental margins. *Geology*, 14, 246-250.

Martin, A.K. (2011) Double saloon door tectonics in the Japan Sea, Fossa Magna, and the Japanese Island Arc. *Tectonophysics*, 498, 45-65.

- Nishizawa, A. and Asada, A. (1999) Deep crustal structure of Akita, Eastern Margin of the Japan Sea, deduced from Ocean Bottom Seismographic Measurements. *Tectonophysics*, 306, 199-216.
- Northrup, C.J., Royden, L.H. and Burchfiel, B.C. (1995) Motion of the Pacific plate relative to Eurasia and its potential relation to Cenozoic extension along the eastern margin of Eurasia. *Geology*, 23, 719-722.
- Okamura, Y. (2000) Inversion tectonics along the eastern margin of the Japan Sea. *Jour. Assco. Petrol. Tech. Japan*. 65(1), 40-47 (in Japanese with English abstract).
- Otofujii, Y., Matsuda, T. and Nohda, S. (1985) Paleomagnetic evidence for the Miocene counter-clockwise rotation of Northeast Japan-rifting process of the Japan Arc. *Earth Planet. Sci. Lett.*, 75, 265-277.
- Otsuki, K., (1982) Composite model" on the consumingt plate boundary tectonics. *Kouzou Chishitsu Kenkyuu Kaishi*, 27, 127-142 (in Japanese with no English abstract).
- Otsuki, K. and Ehiro, M. (1992) Cretaceous left-lateral faulting in Northeast Japan and its bearing on the origin of geologic structure of Japan. *Jour. Geol. Soc. Japan*, 98, 1097-1112 (in Japanese with English abstract).
- Shao, G., Li, X., Ji, C. and Maeda, T. (2011) Focal mechanism and slip history of the 2011 Mw9.1

off the Pacific coast of Tohoku Earthquake, constrained with teleseismic body and surface waves. *Earth Planets Space*, 63, 559-564.

Suwa, Y, Miura, S., Hasegawa, A., Sato, T. and Tachibana, K. (2006) Interplate coupling beneath NE Japan inferred from three-dimensional displacement field. *Jour., J. Geophys. Res.*, 111, B04402, doi:10.1029/2004JB003203.

Taguchi, K. (1960) On the lower formation of the Neogene Tertiary in the Dewa Hilly Land (Geological studies of the "Dewa Geosyncline" Northern Honshu-II). *Jour. Geol. Soc. Japan*, 66, 102-112 (in Japanese with English abstract).

Takahashi, M. (2006) Tectonic boundary between Northeast and Southwest Japan Area during Japan Sea opening. *Jour. Geol. Soc. Japan*, 112, 14-32.

Takahashi, N., Kodaira, S., Tsuru, T., Park, J., Kaneda, Y., Suyehiro, K., Kinoshita, H., Abe, S., Nishino, M. and Hino, R. (2004) Seismic structure and seismogenesis off Sanriku region, northeastern Japan. *Geophys. Jour. Int.*, 159, 129-145.

Ten Brink, U. S., and Zvi, B. A. (1989) The anatomy of a pull-apart basin: seismic reflection observations of the Dead Sea Basin. *Tectonics* 8, 333–350.

Uchida, N. and Matsuzawa, T (2013). Pre- and postseismic slow slip surrounding the 2011 Tohoku-oki earthquake rupture. *Earth and Planetary Science Letters*, 374, 81-91.

Yagi, Y. and Fukahata, Y. (2011) Rupture process of the 2011 Tohoku-oki earthquake and absolute elastic strain release. *Geophys. Res. Lett.*, 38, L19307, doi:10.1029/2011GL 048701.

Yoshida, K., Miyakoshi, K. and Irikura, K. (2011) Source process of the 2011 off the Pacific coast of Tohoku Earthquake inferred from waveform inversion with long-period strong-motion records. *Earth Planets Space*, 63, 577-582.

Yoshida, Y., Ueno, H., Muto, D. and Aoki, S. (2011) Source process of the 2011 off the Pacific coast of Tohoku Earthquake with the combination of teleseismic and strong motion data. *Earth Planets Space*, 63, 565-569.

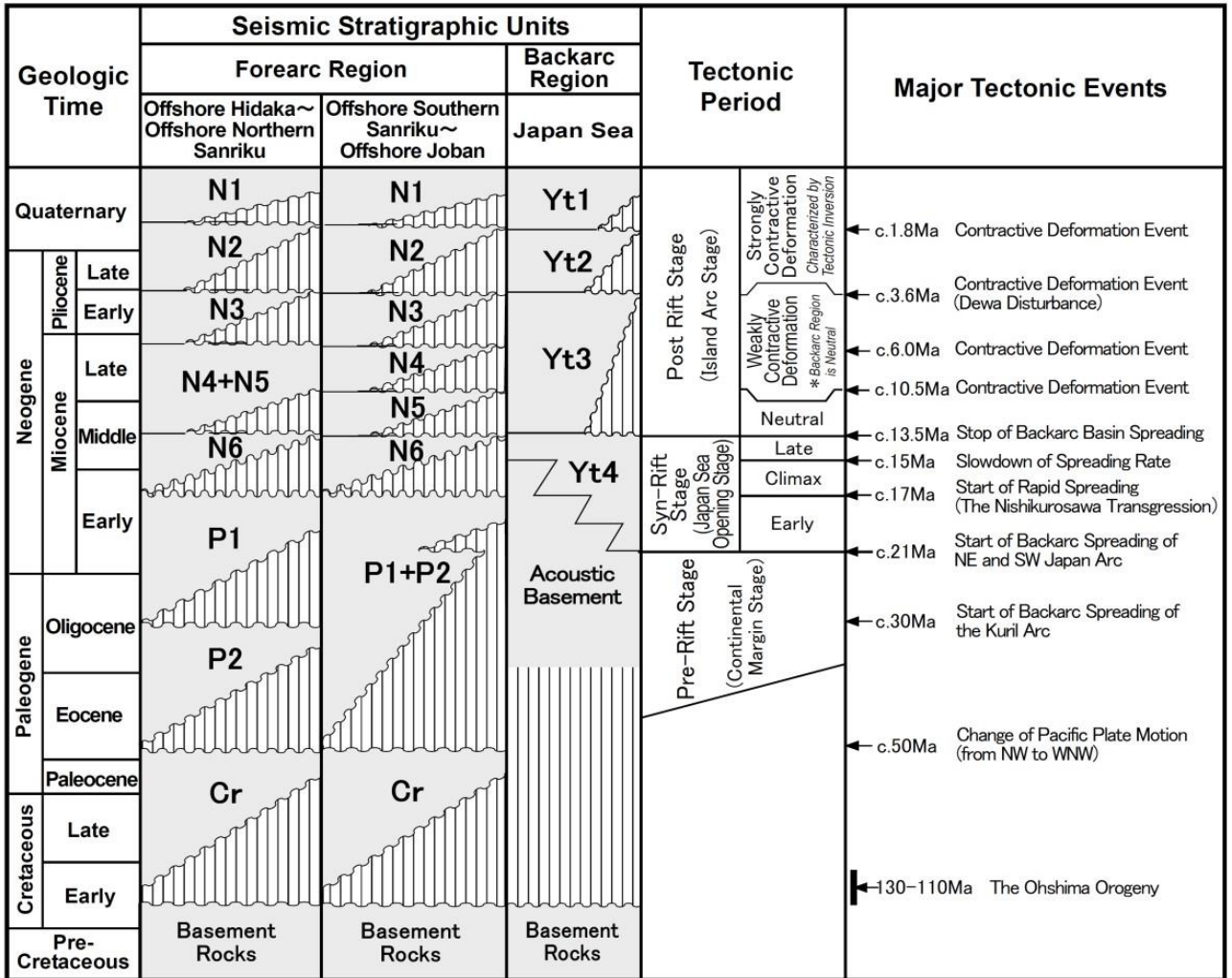


Fig. S1 Regional stratigraphic correlation chart of the surrounding ocean region of the NE Japan Arc (adapted from Baba, 2017).

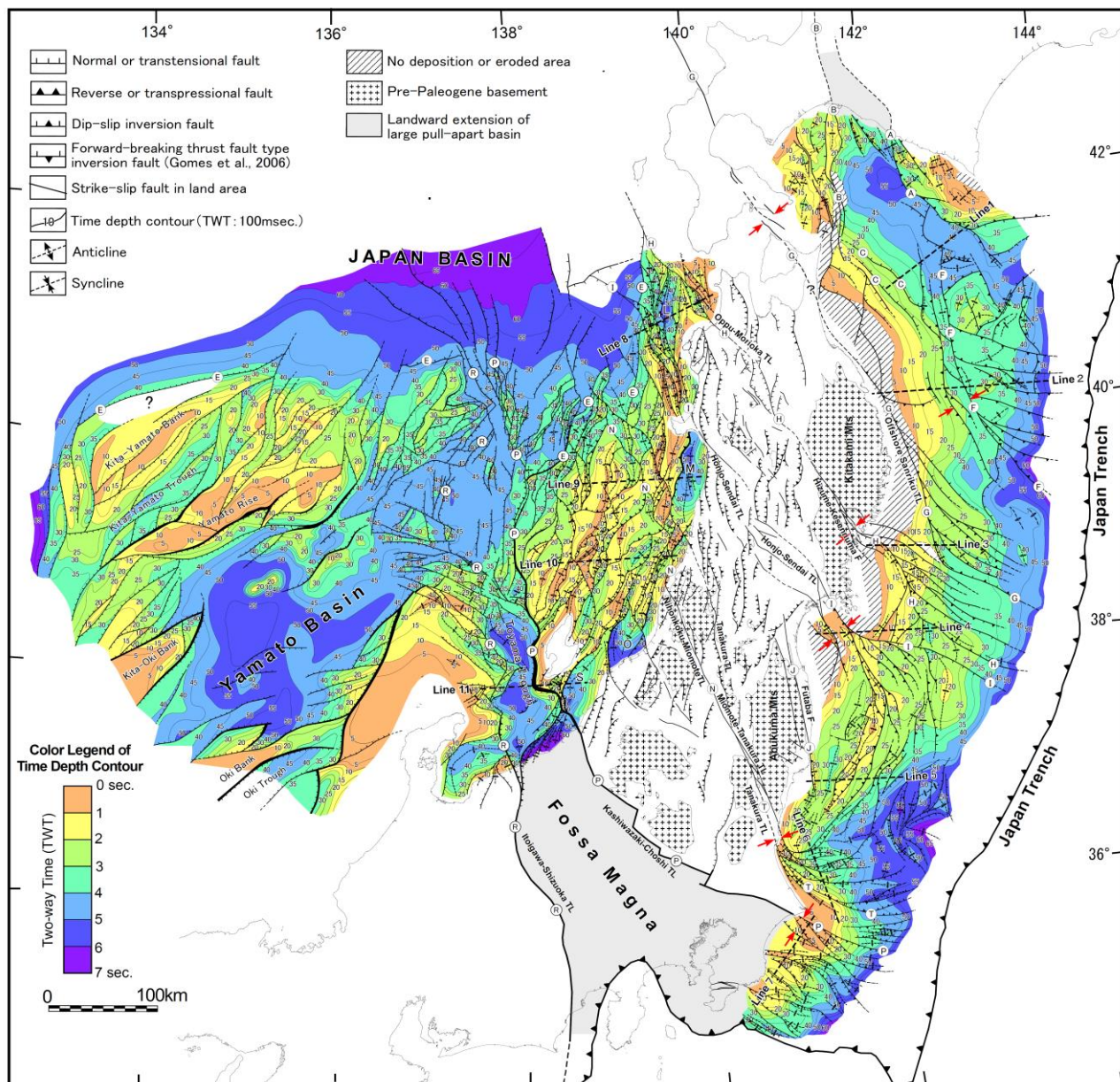


Fig. S2 Time contour map of the top of the P1 seismic stratigraphic unit in the forearc region and the top of the acoustic basement in the backarc region of the NE Japan Arc (adapted from Baba, 2017). The geological age of this map corresponds approximately to the start of the Climax Syn-ryft stage (see Fig. S1). The fault symbols are the same as those in Fig. 2. Small red arrows are the measuring point of maximum width of the large transcurrent faults.

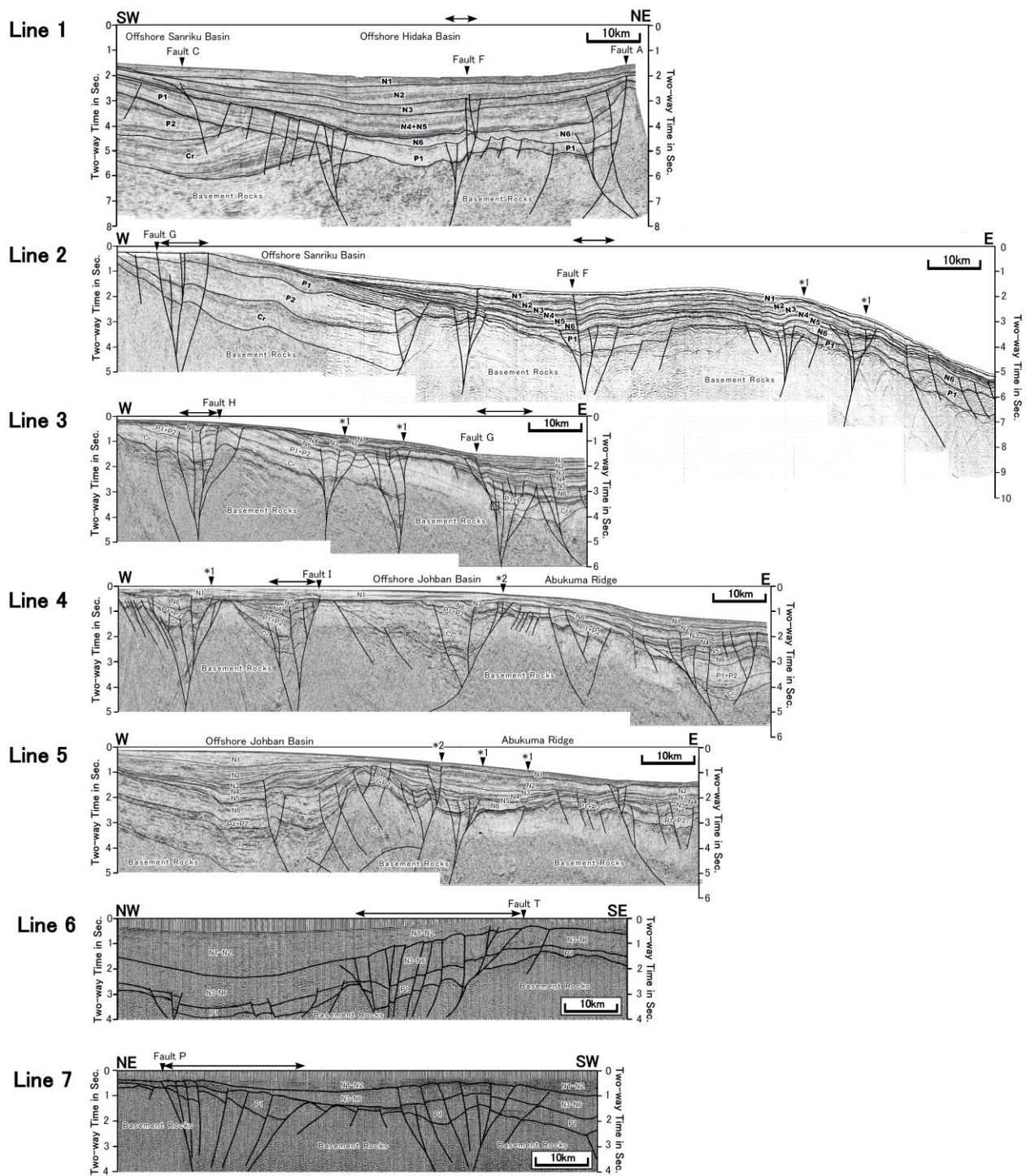


Fig. S3A Typical seismic section of the NE Japan forearc region. The locations of the seismic sections are shown in Fig. S2. *1 is the branch fault of the imbricate fan and *2 is the western margin fault of the Abukuma Ridge (adapted from Baba, 2017). On Lines 6 and 7, we could identify only three seismic units (P1, N6-N3 and N2-N1) because of poor seismic resolution, and the geological age of P1 unit is confined to the Early Miocene because of non-deposition of the Oligocene. The arrow marks at the top of the figure indicate location and width of the flower structure of large transcurrent faults.

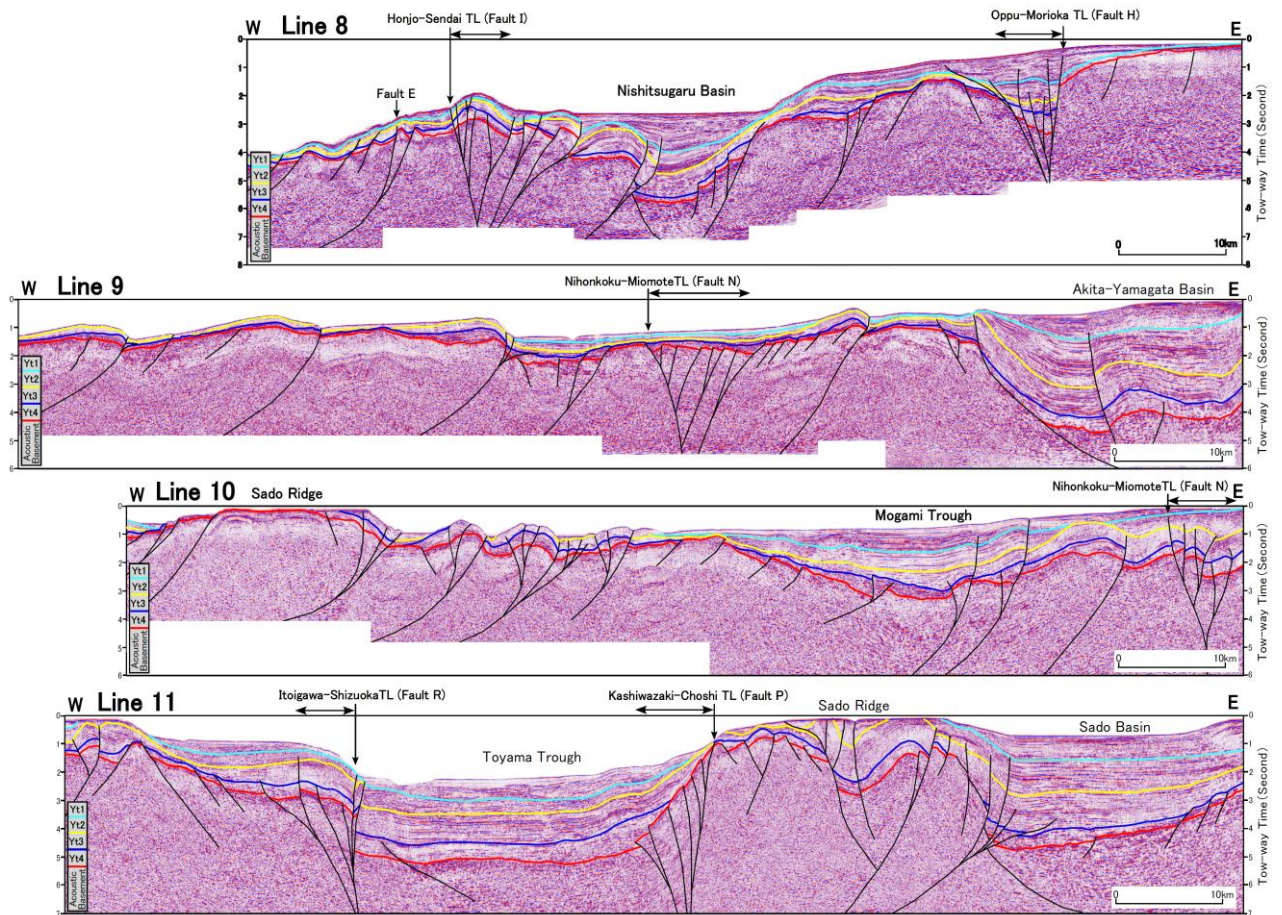


Fig. S3B Typical seismic section of the NE Japan backarc region (adapted from Baba, 2017). The locations of the seismic survey lines are shown in Fig. S2. The arrow marks at the top of the figure indicate location and width of the flower structure of large transcurrent faults.

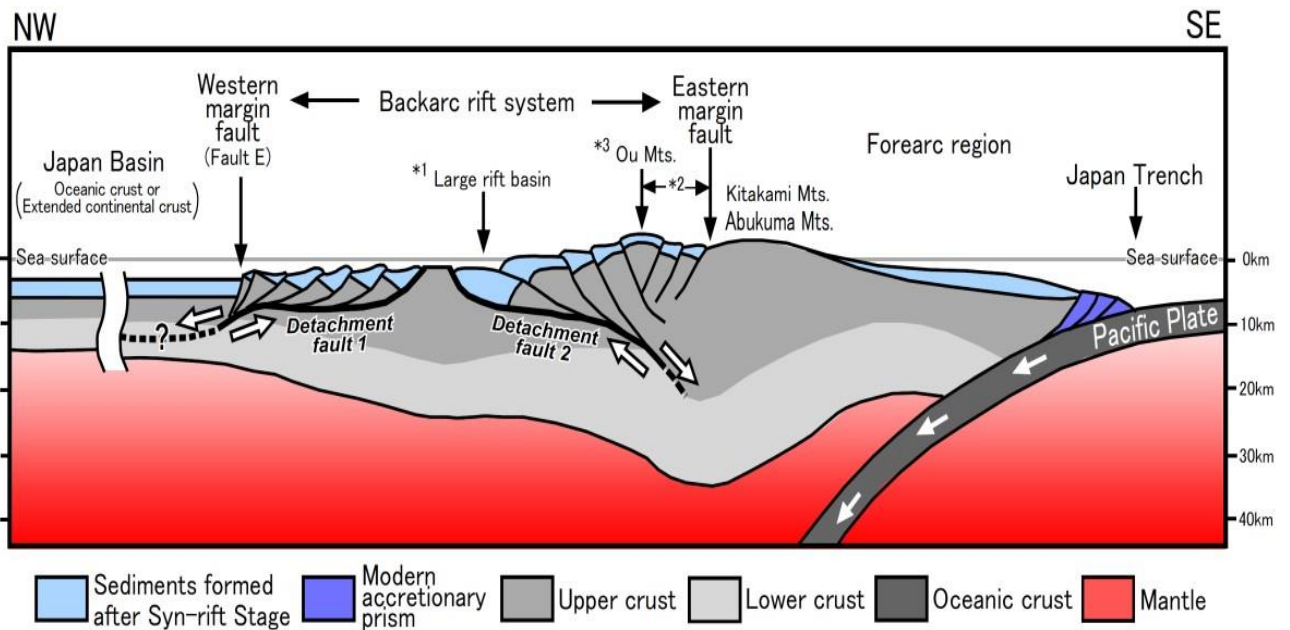


Fig. S4 NW-SE schematic cross section of the NE Japan Arc from the forearc region to the Japan Basin. *1 represents large rift basins such as the Nishitsugaru, the Akita-Yamagata, Niigata, and Sado Basins (see Fig. S2), *2 is the antithetic fault system developed along the eastern margin of the backarc rift system, and 3* is the pop-up structure that forms the Ou mountains. The deep crust structure was modified from Nishizawa and Asada (1999), Iwasaki et al. (2001), and Takahashi et al. (2004). The subtle contractive deformations are often recognized along "Fault E", but most of them have an unmappable scale on seismic records.

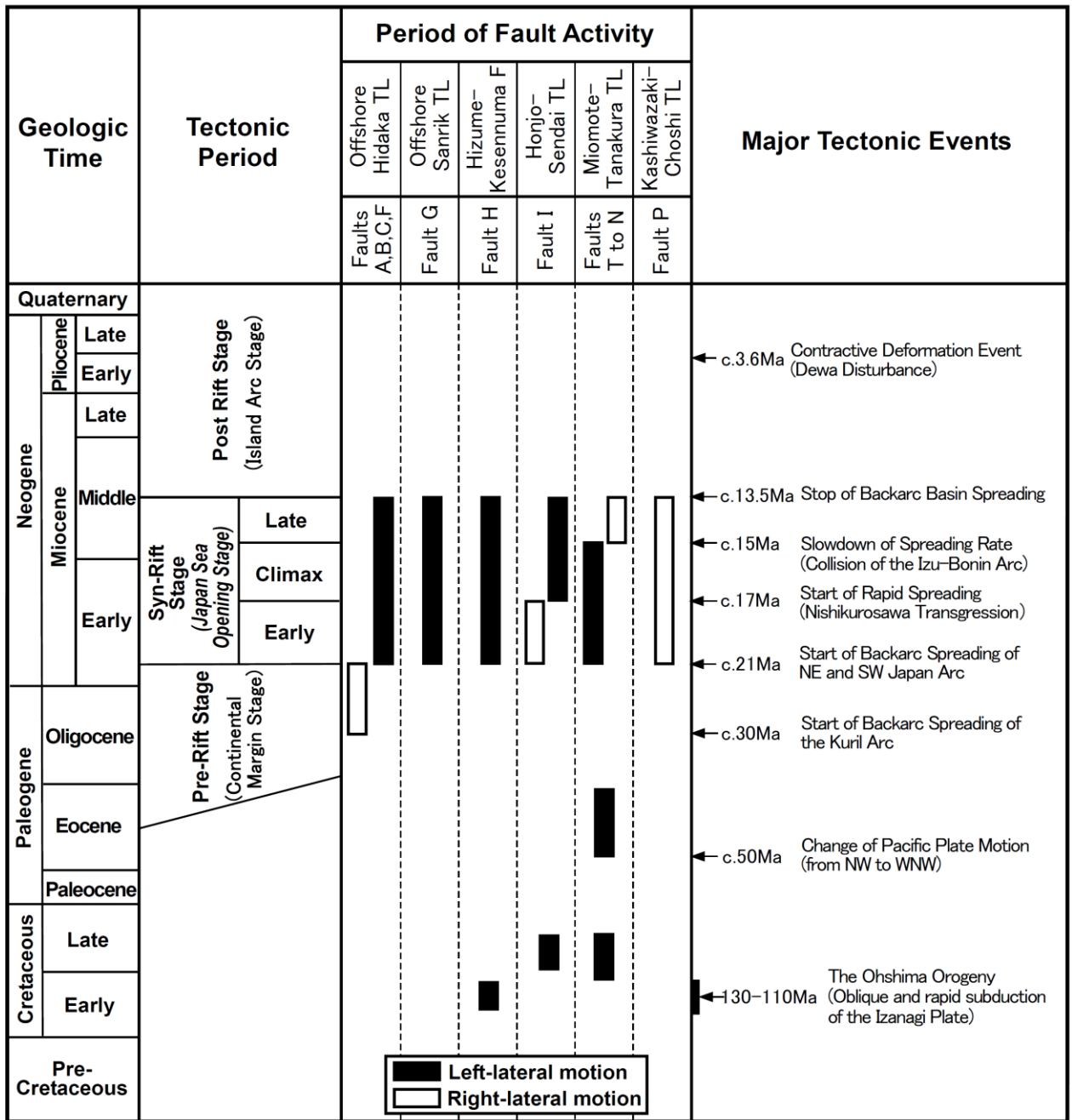


Fig. S5 Fault movement history of large transcurrent faults. Tectonic period and major tectonic events are based on Fig. S1.

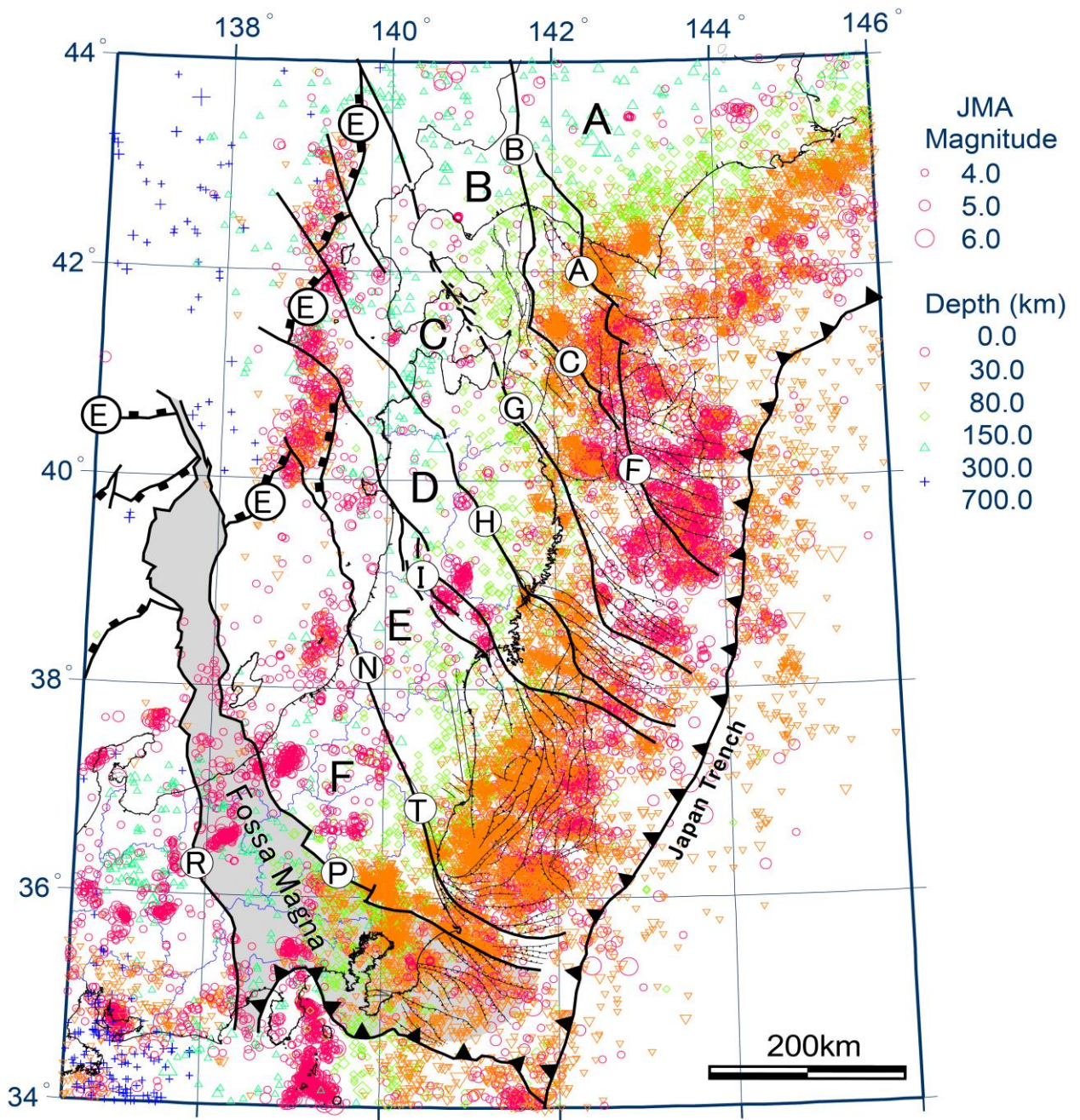


Fig. S6 Distribution of earthquakes greater than Mj 4.0 from March 9, 1931, to March 8, 2011. The earthquake depth ranges from 1.0 to 700.0 km. The earthquake dataset was obtained from JMA earthquake catalog.

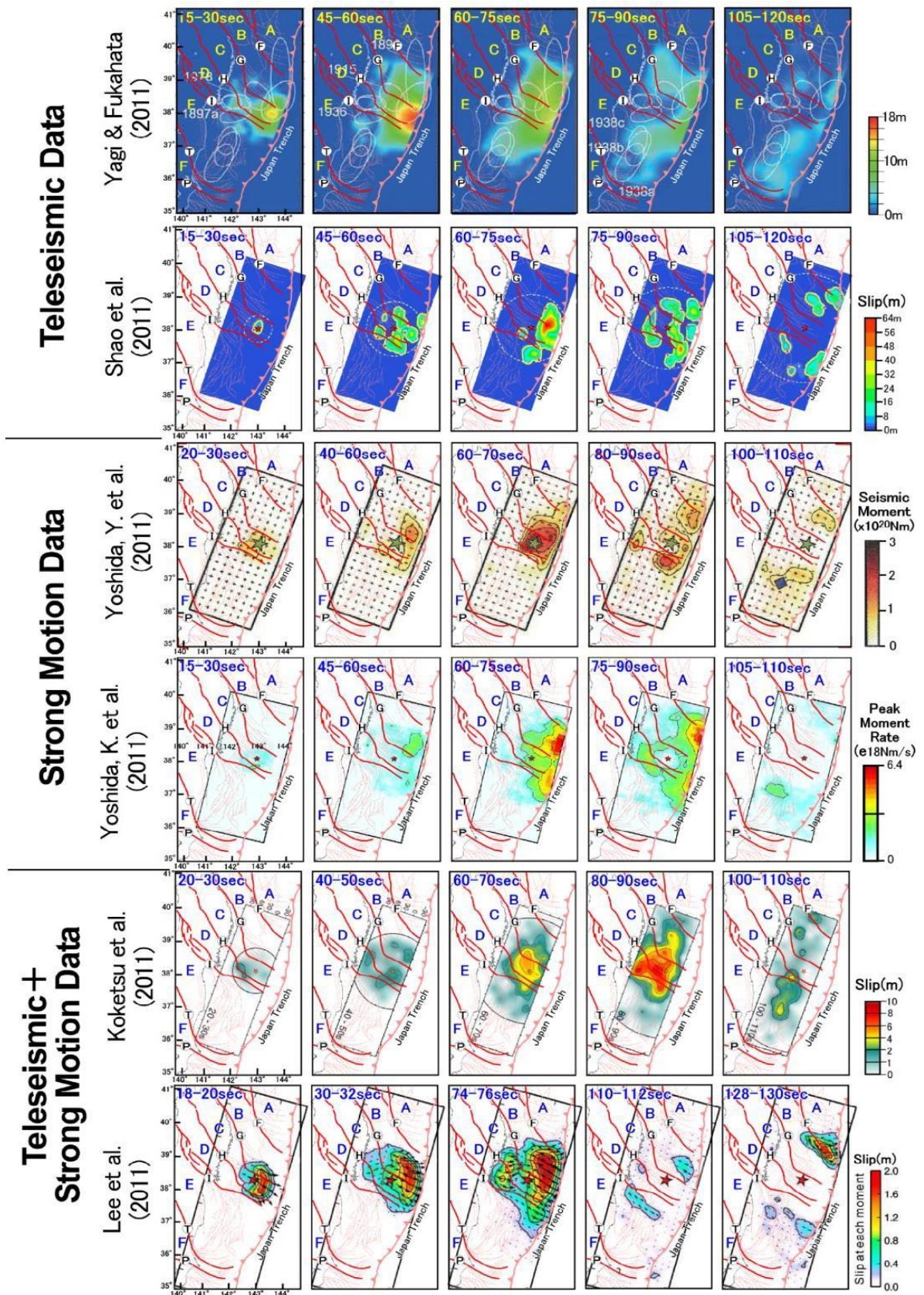


Fig. S7 Snapshots of rupture propagation models superimposed on the fault distribution map of Fig. 2. The symbols are the same as those in Fig. 2.

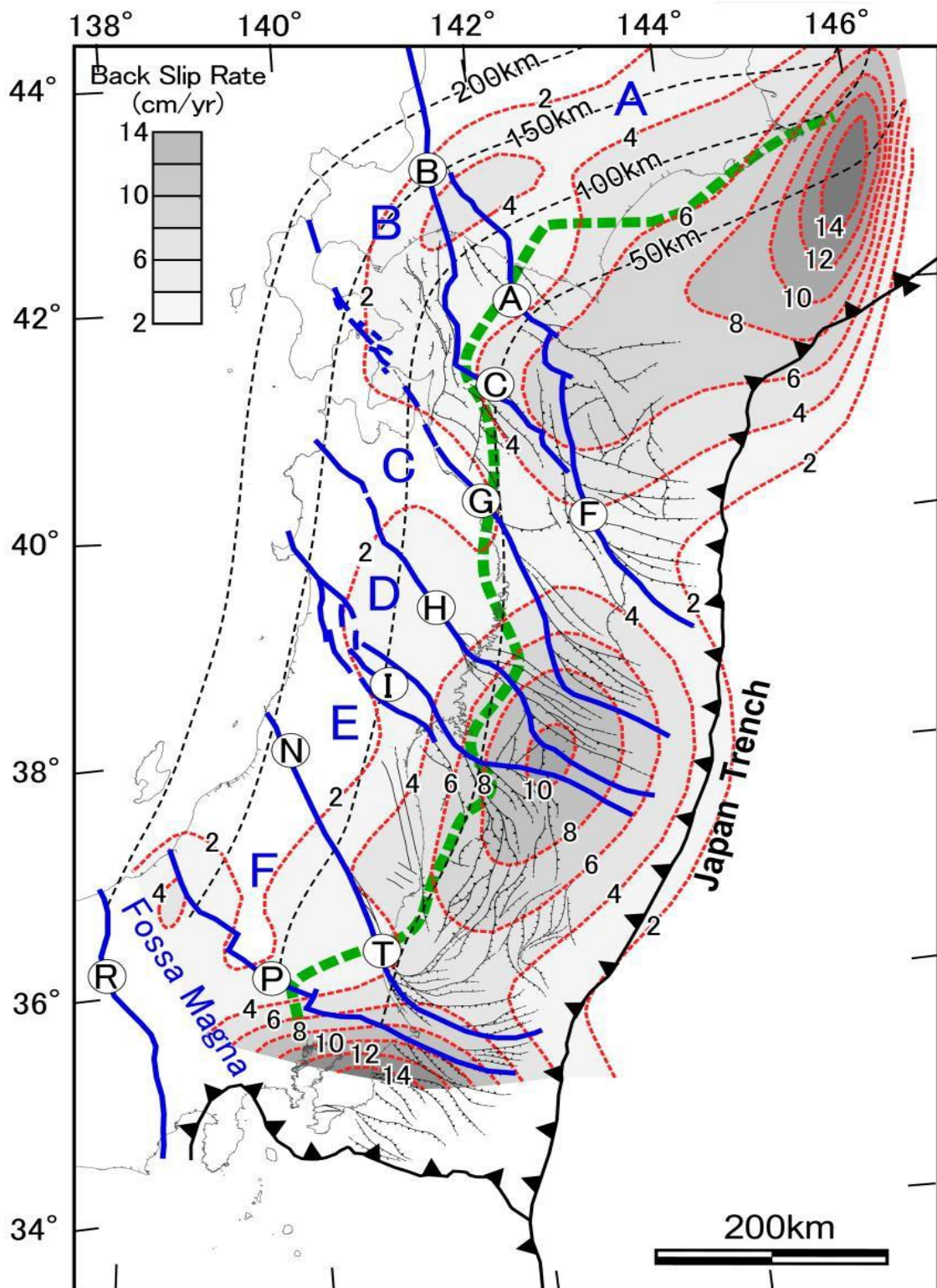


Fig. S8 Distribution of the back slip rate estimated by Suwa et al. (2006) overlaid on the fault distribution map of Figs. 1 and 2. The contour interval is 2 cm/yr and black dashed lines indicate the slab depth every 50 km. The green dashed line is the downdip limit of interplate earthquakes of Uchida and Matsuzawa (2013). The fault symbols are the same as those in Fig. 2.